^{68}Ga-NOTA-PRGD2 PET/CT for Integrin Imaging in Patients with Lung Cancer

Kun Zheng*[1], Naixin Liang*[2], Jingjing Zhang*[1], Lixin Lang[3], Wei Zhang[1], Shanqing Li[2], Jun Zhao[4], Gang Niu[3], Fang Li[1], Zhaohui Zhu[1], and Xiaoyuan Chen[3]

[1]Department of Nuclear Medicine, Peking Union Medical College Hospital, Chinese Academy of Medical Sciences and Peking Union Medical College, Beijing, China; [2]Department of Thoracic Surgery, Peking Union Medical College Hospital, Chinese Academy of Medical Sciences and Peking Union Medical College, Beijing, China; [3]Laboratory of Molecular Imaging and Nanomedicine (LOMIN), National Institute of Biomedical Imaging and Bioengineering, National Institutes of Health, Bethesda, Maryland; and [4]Department of Thoracic Surgery, Cancer Hospital of Chinese Academy of Medical Sciences and Peking Union Medical College, Beijing, China

This study was designed to assess the diagnostic value of ^{68}Ga-NOTA-PRGD2 (NOTA-PRGD2 is NOTA-PEG4-E[c(RGDfK)]$_2$) PET/CT in lung cancer. **Methods:** Ninety-one patients (48 men and 43 women; age, 22–82 y) with suspected lung lesions on CT were enrolled with informed consent. Immediately after intravenous injection of 117.7 ± 37.7 MBq of ^{68}Ga-NOTA-PRGD2, 15 patients underwent dynamic whole-body PET/CT scans for 1–2 h, and the remaining 76 patients underwent whole-body PET/CT scans at 30 ± 10 min after bolus injection. Each patient also underwent standard ^{18}F-FDG PET/CT for comparison. **Results:** No side effect was found after ^{68}Ga-NOTA-PRGD2 injection. ^{68}Ga-NOTA-PRGD2 was rapidly cleared from the blood pool and primarily excreted through the urinary system. The standardized uptake values of proven malignancies were significantly higher than those of the benign ones. With an average standardized uptake value of greater than 1.3 being considered malignant, the sensitivity, specificity, and accuracy of ^{68}Ga-NOTA-PRGD2 PET/CT in diagnosing lung cancer were 83.8% (57/68), 91.3% (21/23), and 85.7% (78/91), respectively. The diagnostic value of ^{68}Ga-NOTA-PRGD2 for lung cancer is comparable to that of ^{18}F-FDG PET/CT. However, ^{68}Ga-NOTA-PRGD2 PET/CT is more specific than ^{18}F-FDG PET/CT in assessing lymph node metastasis, with positive and negative predictive values of 90.0% (27/30) and 93.8% (121/129), respectively, whereas those of ^{18}F-FDG PET/CT were 30.2% (29/96) and 90.5% (57/63), respectively. **Conclusion:** This study indicates the efficacy of ^{68}Ga-NOTA-PRGD2 PET/CT in lung cancer diagnosis. ^{68}Ga-NOTA-PRGD2 PET/CT shows significant advantage over ^{18}F-FDG PET/CT in judging metastatic lymph nodes with higher specificity.

Key Words: integrin; ^{68}Ga-NOTA-PRGD2; PET/CT; lung cancer; lymph node metastasis

J Nucl Med 2015; 56:1823–1827
DOI: 10.2967/jnumed.115.160648

The integrin family consists of 24 different heterodimerized transmembrane receptors, which play important roles in many physiologic and pathologic processes including cell survival, growth, differentiation, migration, inflammatory responses, platelet aggregation, tissue repair, and tumor invasion (*1*). Among them, integrin receptor $\alpha_v\beta_3$ is one of the key molecules participating in tumor angiogenesis, invasion, and metastasis (*2–4*). On the basis of the key role it plays in oncology and its easy accessibility as a cell surface receptor, integrin $\alpha_v\beta_3$ has been intensively investigated as a target for both therapeutic and diagnostic uses in various malignancies (*5–8*).

Several extracellular matrix proteins interact with integrin $\alpha_v\beta_3$ through the arginine-glycine-aspartic acid (RGD) tripeptide sequence, and thus cyclic RGD peptides with various modifications have been labeled with ^{99m}Tc (*9*) and ^{111}In (*10*) for SPECT imaging and with ^{18}F (*11*), ^{64}Cu (*12*), ^{68}Ga (*13,14*), and ^{89}Zr (*15*) for PET imaging. The peptide modifications have included dimerization and polymerization of up to 8 cyclic RGD peptide units to increase binding affinity and the attachment of polar functional groups, such as sugar and polyethylene glycol (PEG), to increase renal excretion (*16,17*).

One clinical study reported the use of ^{68}Ga-labeled RGD monomer in pediatric patients with moyamoya disease (*18*). Compared with the monomer, the dimeric RGD peptide binds the receptor in a divalent manner and is thus more preferable in targeting integrin-expressing cells both in vitro and in mouse models. Therefore, dimeric RGD is expected to have more intense uptake and more prolonged retention than the monomeric counterpart in integrin-expressing tumors (*19,20*).

Lung cancer is one of the leading causes of cancer mortality worldwide. PET imaging using ^{18}F-FDG has become the standard of care in the initial management of patients with lung cancer, especially non–small cell lung cancer (*21*). However, false-positive ^{18}F-FDG PET/CT results in nodal staging have been shown in patients with coexistent inflammatory or infectious diseases (*22*). Therefore, alternative imaging probes for accurate staging studies are necessary to assess the extent of disease and to determine appropriate treatment. In this study, we investigated the diagnostic value of a ^{68}Ga-labeled RGD dimer, ^{68}Ga-NOTA-PRGD2 (NOTA-PRGD2 is NOTA-PEG4-E[c(RGDfK)]$_2$), for lung cancer using PET/CT.

Received Sep. 16, 2015; revision accepted Sep. 21, 2015.
For correspondence or reprints contact either of the following:
Xiaoyuan Chen, National Institutes of Health, 35A Convent Dr., GD937, Bethesda, MD 20892-3759.
E-mail: shawn.chen@nih.gov
Zhaohui Zhu, Department of Nuclear Medicine, Peking Union Medical College Hospital, Chinese Academy of Medical Sciences and Peking Union Medical College, Beijing 100730, China.
E-mail: zhuzhh@pumch.cn
*Contributed equally to this work.
Published online Oct. 1, 2015.

MATERIALS AND METHODS

This clinical study was approved by the Institutional Review Board (IRB) of the Peking Union Medical College Hospital, Chinese Academy of Medical Sciences and Peking Union Medical College (IRB protocol S-417). All subjects signed a written informed consent form. This study was registered at the National Institutes of Health ClinicalTrials.gov (NCT01737112).

Volunteers and Patients

To validate the safety of ^{68}Ga-NOTA-PRGD2 PET/CT, 7 healthy volunteers (3 men and 4 women; age, 38–65 y; mean age ± SD, 48 ± 9 y) were enrolled (the supplemental data provides more details; supplemental materials are available at http://jnm.snmjournals.org). To study the diagnostic value of ^{68}Ga-NOTA-PRGD2 PET/CT, 91 patients (48 men and 43 women; age, 22–82 y; 56.5 ± 14.9 y) with suspected lung lesions according to CT were enrolled. The inclusion criteria were age 18 y or older, identified with lung lesion by CT in suspicion of primary lung cancer, and ability to provide basic information and sign the written informed consent form. The exclusion criteria included claustrophobia, possible pregnancy, lactation, kidney or liver failure, and inability to fulfill the study. Of the 91 patients recruited, 68 patients (36 men and 32 women; age, 30–82 y; 58.7 ± 12.9 y) were diagnosed as having lung cancer, based on the pathologic result of surgical removal or biopsy. Twenty-three benign diagnoses (12 men and 11 women; age, 22–76 y; 50.1 ± 18.6 y) were made on both pathologic results (n = 19) and follow-up (n = 4). The follow-up CT or PET/CT reexaminations in the 4 patients were obviously diminished after antiinflammatory treatment and disappeared after 6 mo to 1 y. The detailed diagnostic information of all patients is listed in Table 1.

^{68}Ga-NOTA-PRGD2 Preparation

^{68}Ga-NOTA-PRGD2 was synthesized in a sterile hot cell. The precursor NOTA-PRGD2 (*14*) was dissolved in deionized water to 1 μg/μL and stored at 4°C before use. Fresh ^{68}Ga was eluted into 3 tubes (~1.3 mL each) from the ^{68}Ge/^{68}Ga generator (ITG Co.) using 4 mL of 0.05 M HCL (J.T. Baker). A pipette (Thermo Co., USA) was used to draw 1,000 μL of $^{68}GaCl_3$ eluent from the middle tube, and the radioactivity was measured. The solution was then mixed with 50 μL of 1.25 M NaOAc and 40 μL of stored precursor. After shaking, the mixture was kept in a 100°C metal heater (Gingko) for 10 min. After the product was cooled down to room temperature, a 0.22-μm aseptic filtration membrane was used for purification. Radio–thin-layer chromatography (Bioscan) was used to test the radiochemical purity with CH_3OH:NH_4OAc (v/v 1:1) as the developing solution. The radiochemical purity of the product ^{68}Ga-NOTA-PRGD2 exceeded 97%.

TABLE 1
Patient Information and Diagnosis

Demographic or clinical characteristic	*n*
Age (y)	
Range	22–82
Mean ± SD	56.5 ± 14.9
Sex	
Male	48
Female	43
Diagnosis	91
Malignant	68
Adenocarcinoma	45
Squamous cell carcinoma	17
Adenosquamous carcinoma	3
Neuroendocrine carcinoma (SCLC)	3
Benign	23
Granuloma	8
Chronic inflammation	9
Tuberculosis	4
Lipoma	1
Hamartoma	1

Examination Procedures

A Siemens Biograph 128 mCT X scanner was used for ^{68}Ga-NOTA-PRGD2 PET/CT. Volunteers and patients were asked to urinate right before examination. For 15 patients, after the whole-body low-dose CT scan (140 kV; 35 mA; pitch, 1:1; layer, 5 mm; layer spacing, 3 mm; matrix, 512 × 512; field of view, 70 cm), approximately 111 MBq (3 mCi) of ^{68}Ga-NOTA-PRGD2 were injected intravenously, followed by immediate serial whole-body dynamic PET acquisitions. The duration was 3 s/bed position for the 1–8 phases, 6 s/bed position for the 9–14 phases, 60 s/bed position for the 15–17 phases, 120 s/bed position for the next several phases, and the last phase lasted for 240 s/bed position. The whole-body images were obtained in sequence, and the total scanning lasted for 1–2 h based on the patient's height and number of phases. The other 76 patients underwent ^{68}Ga-NOTA-PRGD2 PET/CT scans at 30 ± 10 min after injection.

Except for 1 patient with a benign lesion, all the other 90 patients underwent standard routine ^{18}F-FDG PET/CT within 1 wk. Patients were asked to fast for at least 4 h before the examination, and the blood glucose levels were below 6.4 mM. After injection of approximately 7.4 MBq of ^{18}F-FDG per kilogram, the patients were asked to rest quietly in a warm and dark room for about 1 h. Then, the patients underwent low-dose CT and PET scans from the pelvic bottom to the skull base. A scan usually included 5 or 6 bed positions according to the patient's height, and each bed position lasted for 2 min.

Integrin Immunohistochemical Staining

Representative tumor and lymph node samples were fixed with 10% neutral-buffered formalin and embedded in paraffin. Five-micrometer-thick tissue sections were blocked with endogenous peroxidase using 3% H_2O_2 for 20 min. Sections were then washed 3 times with phosphate-buffered saline briefly in a buffer containing 1% polymerized bovine serum albumin and incubated with mouse antihuman monoclonal antibody against human integrin $\alpha_v\beta_3$ (1:200; SC-7312 [Santa Cruz Biotechnology]) at 37°C for 2 h. After being washed with phosphate-buffered saline, each section was incubated with horseradish peroxidase–conjugated antigoat IgG for 60 min at room temperature. Diaminobenzidine was used as the chromogen, and hematoxylin and eosin counterstaining was performed. Six fields were randomly selected from each section and observed using a light microscope (BX41; Olympus).

Data Analysis

The same physician measured all images with the same standard in the final analysis. A Siemens workstation (MultiModality Workplace) was used for postprocessing. The volume of interest of 15 normal organs/tissues and concerned lesions were drawn on the last set of the serial images, and the software automatically obtained the radioactivity concentration and standardized uptake value (SUV) in the volumes of interest. Prism 5.0 software (GraphPad Software, Inc.) was used for statistical analysis. The same physician compared and measured the ^{68}Ga-NOTA-PRGD2 and ^{18}F-FDG uptake in the lesions

side by side. A receiver-operating-characteristic curve was used to set the threshold for diagnosis of lung cancer. The Student *t* test was used to compare the SUVs of different groups. The *Z* test was used to compare the performance of ^{68}Ga-NOTA-PRGD2 and ^{18}F-FDG PET/CT in evaluating lung cancer. A *P* value of less than 0.05 was considered statistically significant.

RESULTS

Lung Cancer Evaluation

The biodistribution and dosimetry studies in healthy volunteers showed predominant renal clearance of ^{68}Ga-NOTA-PRGD2 and comparable total-body effective dose to that from routine ^{18}F-FDG (more details are provided in the supplemental materials). The low background in the lung region allows the detection of lung lesions with high target-to-background ratio. Moreover, the activity in the heart and mediastinum vasculature faded away quickly, which facilitates easy recognition of abnormal lymph nodes. All positive lesions, including primary tumors, lymphatic and bone metastases, and benign foci could be clearly observed at 30–45 min after intravenous injection of ^{68}Ga-NOTA-PRGD2 (Fig. 1). The lesions with prominent ^{68}Ga-NOTA-PRGD2 uptake appeared to be integrin $\alpha_v\beta_3$–positive.

In the ^{68}Ga-NOTA-PRGD2 PET/CT images of the patients, the average SUV (SUV_{avg}) and maximum SUV (SUV_{max}) of malignances at 30 min after injection were 2.12 ± 1.30 and 3.66 ± 2.87, respectively, which were significantly higher than those of the benign ones (SUV_{avg} = 0.94 ± 0.43 and SUV_{max} = 1.57 ± 0.71, $P < 0.05$). The mean SUV of normal lung tissue was 0.31 ± 0.19, and the mean SUV of normal aortic arch was 0.85 ± 0.44. Using the receiver-operating-characteristic curve and area under the curve of SUV data of ^{68}Ga-NOTA-PRGD2 PET/CT, we determined a threshold of 1.3 for SUV_{avg} and 2.0 for SUV_{max}. The sensitivity, specificity, and accuracy of ^{68}Ga-NOTA-PRGD2 PET/CT in the diagnosis of lung cancer were 83.8% (57/68), 91.3% (21/23), and 85.7% (78/91), respectively, using a cutoff value of 1.3 for SUV_{avg}. The minimal size of detected tumor was 7.5 mm as measured on the CT images using a cutoff value of 1.3 for SUV_{avg}. When SUV_{max} with a cutoff value of 2.0 was used, the sensitivity, specificity, and accuracy of ^{68}Ga-NOTA-PRGD2 PET/CT in the diagnosis of lung cancer were 80.9% (55/68), 82.6% (19/23), and 81.3% (74/91), respectively. For ^{18}F-FDG PET/CT, with a cutoff SUV_{avg} value of 2.0, the sensitivity, specificity, and accuracy were 86.8% (59/68), 69.6% (16/23), and 82.4% (75/91), respectively. With an SUV_{max} cutoff value of 3.0, the sensitivity, specificity, and accuracy of ^{18}F-FDG PET/CT in the diagnosis of lung cancer were 85.3% (58/68), 69.6% (16/23), and 81.3% (74/91), respectively. The critical ratio *z* for comparing ^{68}Ga-NOTA-PRGD2 and ^{18}F-FDG PET/CT in evaluating lung cancer was 1.033 for SUV_{avg} (P = 0.30) and 0.077 for SUV_{max} (P = 0.94).

Both SUV_{avg} and SUV_{max} of ^{18}F-FDG were significantly higher than those of ^{68}Ga-NOTA-PRGD2 ($P < 0.0001$). There was no significant correlation between the ^{18}F-FDG uptake and the ^{68}Ga-NOTA-PRGD2 accumulation. There was no significant difference in ^{68}Ga-NOTA-PRGD2 accumulation and ^{18}F-FDG uptake in primary lung lesions with or without metastatic lymphonodus (P = 0.87 and 0.86, respectively). The SUV_{avg} and SUV_{max} of adenocarcinoma (n = 43) at 30 min after injection of ^{68}Ga-NOTA-PRGD2 were 1.78 ± 1.81 and 3.36 ± 3.42, respectively, and those of squamous cell carcinoma (n = 15) were 2.12 ± 1.05 and 4.43 ± 2.31, respectively. There was no significant difference between the 2 types of tumors (P = 0.63 for SUV_{avg} and P = 0.49 for SUV_{max}). When all the tumors were graded as high, moderate, or low differentiation, no significant correlation was found between SUVs and grade of tumor (correlation coefficient r = 0.208, $P > 0.05$).

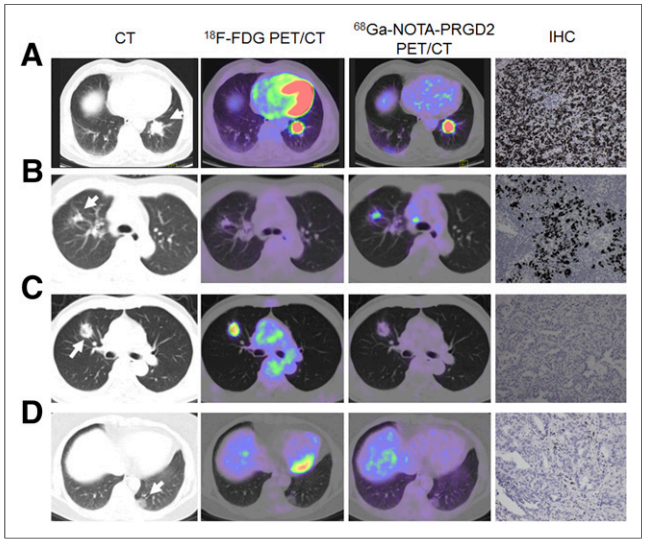

FIGURE 1. CT, ^{18}F-FDG PET/CT, and ^{68}Ga-NOTA-PRGD2 PET/CT images and immunohistochemical (IHC) staining of primary lung cancer. Arrows point to tumor. (A) A 76-y-old man with moderately differentiated adenocarcinoma in inferior lobe of left lung. Lesion is visualized by both ^{18}F-FDG and ^{68}Ga-NOTA-PRGD2 PET, with SUV_{avg}/SUV_{max} of 8.9/14.5 and 4.3/6.1, respectively. Tumor sections show positive integrin $\alpha_v\beta_3$ staining. (B) A 37-y-old woman with highly differentiated adenocarcinoma in superior lobe of right lung. Lesion is visualized only on ^{68}Ga-NOTA-PRGD2 PET with SUV_{avg}/SUV_{max} of 1.7/2.3. Tumor sections show positive integrin $\alpha_v\beta_3$ staining. (C) A 61-y-old woman with highly differentiated adenocarcinoma in superior lobe of right lung. SUV_{avg}/SUV_{max} of ^{18}F-FDG and ^{68}Ga-NOTA-PRGD2 PET were 2.8/4.7 and 0.8/1.3, respectively. Tumor sections show negative integrin $\alpha_v\beta_3$ staining. (D) A 61-y-old woman with highly differentiated adenocarcinoma. CT shows lesion with ground-glass opacity in inferior lobe of left lung. Both ^{18}F-FDG and ^{68}Ga-NOTA-PRGD2 PET show low tracer uptake within lesion with SUV_{avg}/SUV_{max} of 0.7/0.9 and 0.1/0.2, respectively. Tumor sections show sparsely positive integrin $\alpha_v\beta_3$ staining.

Lymph Node Evaluation

For lymph node staging, 38 patients, including 3 cases of chronic inflammation and 35 cases of lung cancer, went through surgery and had confirmed multiregion lymphonodus results. Two hundred nine regions of lymphonodi were recognized from surgery with varied sizes from 0.1 to 2.0 cm. Among them, 50 were too small (<0.5 cm as measured by histopathology) to be identified with the images. In the remaining 159 regions, 35 were metastatic and 124 were normal. As summarized in Table 2, we graded the ^{18}F-FDG uptake and RGD accumulation in 3°: high, moderate, and low. The representative PET images and immunohistochemical staining of lymph nodes are shown in Figure 2. Among the 124 negative lymph nodes, only 3 had low-to-moderate RGD accumulation, but for ^{18}F-FDG, 29 had moderate and 38 had high uptake. In 35 malignant lymph nodes, 8 had very low RGD accumulation, 6 had low-to-moderate accumulation, and 21 had moderate-to-high uptake. If the latter 2 are defined as a sign for metastasis, the positive and negative predictive values of RGD for the assessment of lymph node metastasis were 90.0% (27/30) and 93.8% (121/129), whereas those of ^{18}F-FDG were 30.2%

TABLE 2
^{18}F-FDG Uptake and ^{68}Ga-NOTA-PRGD2 Accumulation in Lymph Nodes

Grade	Nonmetastasis	Metastasis
F0R0	57	5
F1R0	29	2
F2R0	35	1
F0R1	0	1
F2R1	3	5
F2R2	0	21

F stands for ^{18}F-FDG uptake, and 0, 1, and 2 stand for low, moderate, and high, respectively. R stands for extreme ^{68}Ga-NOTA-PRGD2 uptake, and 0, 1, and 2 stand for extremely low, low-to-moderate, and moderate-to-high uptake, respectively.

(29/96) and 90.5% (57/63). Quantitative analysis showed the RGD SUV_{max} of nonmetastatic and metastatic lymphonodi were 0.75 ± 0.75 and 1.93 ± 1.03, respectively ($P < 0.05$), whereas the ^{18}F-FDG SUV_{max} of nonmetastatic and metastatic lymphonodi were 2.30 ± 2.31 and 3.91 ± 2.37, respectively ($P = 0.48$). No apparent correlation between the ^{18}F-FDG uptake or ^{68}Ga-NOTA-PRGD2 accumulation in lymph nodes (Table 2) and the final staging of the 38 patients was found.

DISCUSSION

As a diagnostic study, only a trace amount of NOTA-PRGD2 was used to target the integrin receptor $\alpha_v\beta_3$, so no biologic effect was expected. Indeed, no side effect was found according to the safety data. The results are in accordance with other RGD peptide–based PET tracers such as ^{18}F-galacto-RGD, ^{18}F-AH111585, ^{18}F-RGD-K5, ^{68}Ga-NOTA-RGD, ^{18}F-alfatide, and ^{18}F-FPPRGD2 (*23–29*).

^{18}F-FDG PET has been intensively applied for diagnosis and staging of lung cancer. However, large variations in sensitivity, specificity, and accuracy in lung cancer diagnosis have been reported (*30,31*). The accuracy of ^{18}F-FDG PET for diagnosing lung nodules was extremely heterogeneous (*32*). In this study, the sensitivity of ^{18}F-FDG PET was 86.8%, which is within the range of literature reports. Compared with ^{18}F-FGD PET, ^{68}Ga-NOTA-PRGD2 PET showed lower sensitivity but higher specificity. However, there is no significant difference between the diagnostic values of these 2 tracers. Whether the combination of ^{68}Ga-NOTA-PRGD2 and ^{18}F-FDG will have added value to increase the specificity will need further investigation with a larger patient population.

^{68}Ga-NOTA-PRGD2 PET appears to merit lymph node metastasis assessment, which is important for clinical decision making and surgical planning for lung cancer patients. Although ^{18}F-FDG PET/CT improves the accuracy of N staging, it still cannot replace invasive staging methods, such as mediastinoscopy, mainly because of its relatively low specificity and high uptake in the inflammatory lymph nodes (*33*). In this study, a remarkable improvement of positive predictive value was demonstrated from 30.2% (29/96) in ^{18}F-FDG PET/CT to 90% (27/30) in ^{68}Ga-NOTA-PRGD2 PET/CT. Thirty-five regions of malignant lymphonodi, including the 1 as small as 0.6 cm, were detected by ^{68}Ga-NOTA-PRGD2 PET/CT. Active inflammatory lymphonodi are the main reasons of the false-positive results in ^{18}F-FDG PET/CT (*31*). Most ^{18}F-FDG–avid lymph nodes in acute or chronic inflammation are characterized by lymphoid follicular hyperplasia that cause high ^{18}F-FDG uptake but not necessarily express integrin $\alpha_v\beta_3$. ^{68}Ga-NOTA-PRGD2 PET/CT shows advantages over ^{18}F-FDG PET/CT in the differentiation of malignant and inflammatory lymphonodi. It is also of note that we performed both visual analysis and semiquantitative SUV analysis, and visual analysis is preferred and SUV would be a secondary aid (*34*).

Because RGD peptide tracers bind specifically with integrin $\alpha_v\beta_3$, there have been numerous reports of positive correlation of tracer uptake with the receptor density (*35,36*). We also observed a similar correlation between ^{68}Ga-NOTA-PRGD2 SUVs with immunohistochemical staining results. Because we did not have access to all the tumor tissues, it is thus not possible for us to perform a systematic analysis to answer the question of whether a metastatic lymph node is always integrin-positive. There is also concern about the lymph node lesion size. In this study, 50 of 209 regions of lymphonodi that were smaller than 0.5 cm were directly excluded from the analysis, which may

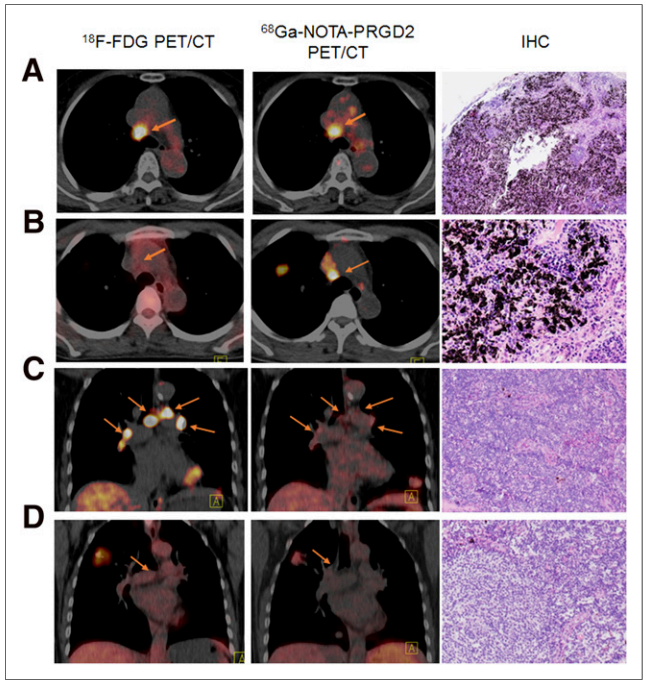

FIGURE 2. ^{18}F-FDG PET/CT and ^{68}Ga-NOTA-PRGD2 PET/CT images and immunohistochemiscal (IHC) staining of lymph nodes within lung region. Arrows point to lymph nodes. (A) A 69-y-old woman with moderately differentiated adenocarcinoma with lymph node metastasis. Both ^{18}F-FDG and ^{68}Ga-NOTA-PRGD2 PET show positive lymph nodes with positive integrin $\alpha_v\beta_3$ staining. (B) A 44-y-old woman with highly differentiated adenocarcinoma with lymph node metastasis. Lymph node is negative on ^{18}F-FDG PET and positive on ^{68}Ga-NOTA-PRGD2 PET with positive integrin $\alpha_v\beta_3$ staining. (C) A 58-y-old woman with adenocarcinoma with no lymph node metastasis. However, ^{18}F-FDG PET shows positive lymph nodes whereas ^{68}Ga-NOTA-PRGD2 PET shows negative result with negative integrin $\alpha_v\beta_3$ staining. (D) A 62-y-old woman with highly differentiated adenocarcinoma with no lymph node metastasis. Both ^{18}F-FDG and ^{68}Ga-NOTA-PRGD2 PET show negative lymph nodes with negative integrin $\alpha_v\beta_3$ staining.

have caused a negative diagnosis in both ^{18}F-FDG and ^{68}Ga-NOTA-PRGD2 scans.

CONCLUSION

^{68}Ga-NOTA-PRGD2 is a safe PET agent that offers good human tolerance and clear images. ^{68}Ga-NOTA-PRGD2 PET/CT has a sensitivity similar to and specificity higher than ^{18}F-FDG PET/CT in the detection and differentiation of lung lesions. Moreover, ^{68}Ga-NOTA-PRGD2 PET/CT shows significant advantage over ^{18}F-FDG PET/CT for N staging of lung cancer, with a remarkable improvement of positive predictive value in the assessment of lymph node metastasis.

DISCLOSURE

The costs of publication of this article were defrayed in part by the payment of page charges. Therefore, and solely to indicate this fact, this article is hereby marked "advertisement" in accordance with 18 USC section 1734. This work was supported in part by the Capital Special Project for Featured Clinical Application (Z121107001012119), the National Natural Science Foundation of China projects (81171369, 81171370, 81371596, and 81271614), the Ministry of Education of China (311037), Young Scientist Research Funding of Peking Union Medical College Hospital (PUMCH2013), and the Intramural Research Program (IRP) of the National Institute of Biomedical Imaging and Bioengineering (NIBIB), National Institutes of Health (NIH). No other potential conflict of interest relevant to this article was reported.

REFERENCES

1. Niu G, Chen X. Why integrin as a primary target for imaging and therapy. *Theranostics.* 2011;1:30–47.
2. Mizejewski GJ. Role of integrins in cancer: survey of expression patterns. *Proc Soc Exp Biol Med.* 1999;222:124–138.
3. Varner JA, Cheresh DA. Integrins and cancer. *Curr Opin Cell Biol.* 1996;8:724–730.
4. Felding-Habermann B, Fransvea E, O'Toole TE, Manzuk L, Faha B, Hensler M. Involvement of tumor cell integrin αvβ3 in hematogenous metastasis of human melanoma cells. *Clin Exp Metastasis.* 2002;19:427–436.
5. Brooks PC, Montgomery AM, Rosenfeld M, et al. Integrin αvβ3 antagonists promote tumor regression by inducing apoptosis of angiogenic blood vessels. *Cell.* 1994;79:1157–1164.
6. Eliceiri BP, Cheresh DA. The role of α_v integrins during angiogenesis: insights into potential mechanisms of action and clinical development. *J Clin Invest.* 1999;103:1227–1230.
7. Chen X, Sievers E, Hou Y, et al. Integrin $\alpha_v\beta_3$-targeted imaging of lung cancer. *Neoplasia.* 2005;7:271–279.
8. Mousa SA. Anti-integrin as novel drug-discovery targets: potential therapeutic and diagnostic implications. *Curr Opin Chem Biol.* 2002;6:534–541.
9. Noiri E, Goligorsky MS, Wang GJ, et al. Biodistribution and clearance of ^{99m}Tc-labeled Arg-Gly-Asp (RGD) peptide in rats with ischemic acute renal failure. *J Am Soc Nephrol.* 1996;7:2682–2688.
10. Ahmadi M, Sancey L, Briat A, et al. Chemical and biological evaluations of an ^{111}In-labeled RGD-peptide targeting integrin $\alpha_v\beta_3$ in a preclinical tumor model. *Cancer Biother Radiopharm.* 2008;23:691–700.
11. Chen X, Park R, Shahinian AH, et al. ^{18}F-labeled RGD peptide: initial evaluation for imaging brain tumor angiogenesis. *Nucl Med Biol.* 2004;31:179–189.
12. Chen X, Liu S, Hou Y, et al. MicroPET imaging of breast cancer α_v-integrin expression with ^{64}Cu-labeled dimeric RGD peptides. *Mol Imaging Biol.* 2004; 6:350–359.
13. Jeong JM, Hong MK, Chang YS, et al. Preparation of a promising angiogenesis PET imaging agent: ^{68}Ga-labeled c(RGDyK)-isothiocyanatobenzyl-1,4,7-triazacyclononane-1,4,7-triacetic acid and feasibility studies in mice. *J Nucl Med.* 2008;49:830–836.
14. Li ZB, Chen K, Chen X. ^{68}Ga-labeled multimeric RGD peptides for microPET imaging of integrin $\alpha_v\beta_3$ expression. *Eur J Nucl Med Mol Imaging.* 2008;35: 1100–1108.
15. Jacobson O, Zhu L, Niu G, et al. MicroPET imaging of integrin $\alpha_v\beta_3$ expressing tumors using ^{89}Zr-RGD peptides. *Mol Imaging Biol.* 2011;13:1224–1233.
16. Dijkgraaf I, Liu S, Kruijtzer JA, et al. Effects of linker variation on the in vitro and in vivo characteristics of an ^{111}In-labeled RGD peptide. *Nucl Med Biol.* 2007;34:29–35.
17. Liu S, Liu Z, Chen K, et al. ^{18}F-labeled galacto and PEGylated RGD dimers for PET imaging of $\alpha_v\beta_3$ integrin expression. *Mol Imaging Biol.* 2010;12:530–538.
18. Choi H, Phi JH, Paeng JC, et al. Imaging of integrin $\alpha_v\beta_3$ expression using ^{68}Ga-RGD positron emission tomography in pediatric cerebral infarct. *Mol Imaging.* 2013;12:213–217.
19. Dijkgraaf I, Yim CB, Franssen GM, et al. PET imaging of $\alpha_v\beta_3$ integrin expression in tumours with ^{68}Ga-labelled mono-, di- and tetrameric RGD peptides. *Eur J Nucl Med Mol Imaging.* 2011;38:128–137.
20. Lang L, Li W, Guo N, et al. Comparison study of [^{18}F]FAl-NOTA-PRGD2, [^{18}F]FPPRGD2, and [^{68}Ga]Ga-NOTA-PRGD2 for PET imaging of U87MG tumors in mice. *Bioconjug Chem.* 2011;22:2415–2422.
21. Chang AJ, Dehdashti F, Bradley JD. The role of positron emission tomography for non-small cell lung cancer. *Pract Radiat Oncol.* 2011;1:282–288.
22. Billé A, Pelosi E, Skanjeti A, et al. Preoperative intrathoracic lymph node staging in patients with non-small-cell lung cancer: accuracy of integrated positron emission tomography and computed tomography. *Eur J Cardiothorac Surg.* 2009;36:440–445.
23. Kim JH, Lee JS, Kang KW, et al. Whole-body distribution and radiation dosimetry of ^{68}Ga-NOTA-RGD, a positron emission tomography agent for angiogenesis imaging. *Cancer Biother Radiopharm.* 2012;27:65–71.
24. Beer AJ, Haubner R, Wolf I, et al. PET-based human dosimetry of ^{18}F-galacto-RGD, a new radiotracer for imaging $\alpha_v\beta_3$ expression. *J Nucl Med.* 2006;47:763–769.
25. Kenny LM, Coombes RC, Oulie I, et al. Phase I trial of the positron-emitting Arg-Gly-Asp (RGD) peptide radioligand ^{18}F-AH111585 in breast cancer patients. *J Nucl Med.* 2008;49:879–886.
26. McParland BJ, Miller MP, Spinks TJ, et al. The biodistribution and radiation dosimetry of the Arg-Gly-Asp peptide ^{18}F-AH111585 in healthy volunteers. *J Nucl Med.* 2008;49:1664–1667.
27. Wan W, Guo N, Pan D, et al. First experience of ^{18}F-alfatide in lung cancer patients using a new lyophilized kit for rapid radiofluorination. *J Nucl Med.* 2013;54:691–698.
28. Mittra ES, Goris ML, Iagaru AH, et al. Pilot pharmacokinetic and dosimetric studies of ^{18}F-FPPRGD2: a PET radiopharmaceutical agent for imaging $\alpha_v\beta_3$ integrin levels. *Radiology.* 2011;260:182–191.
29. Gao S, Wu H, Li W, et al. A pilot study imaging integrin $\alpha_v\beta_3$ with RGD PET/CT in suspected lung cancer patients. *Eur J Nucl Med Mol Imaging.* July 9, 2015 [Epub ahead of print].
30. Freudenberg LS, Rosenbaum SJ, Beyer T, Bockisch A, Antoch G. PET versus PET/CT dual-modality imaging in evaluation of lung cancer. *Radiol Clin North Am.* 2007;45:639–644.
31. Deppen S, Putnam JB Jr, Andrade G, et al. Accuracy of FDG-PET to diagnose lung cancer in a region of endemic granulomatous disease. *Ann Thorac Surg.* 2011;92:428–432.
32. Deppen SA, Blume JD, Kensinger CD, et al. Accuracy of FDG-PET to diagnose lung cancer in areas with infectious lung disease: a meta-analysis. *JAMA.* 2014;312:1227–1236.
33. Iskender I, Kapicibasi HO, Kadioglu SZ, et al. Comparison of integrated positron emission tomography/computed tomography and mediastinoscopy in mediastinal staging of non-small cell lung cancer: analysis of 212 patients. *Acta Chir Belg.* 2012;112:219–225.
34. Hellwig D, Graeter TP, Ukena D, et al. ^{18}F-FDG PET for mediastinal staging of lung cancer: which SUV threshold makes sense? *J Nucl Med.* 2007;48:1761–1766.
35. Beer AJ, Haubner R, Sarbia M, et al. Positron emission tomography using [^{18}F]galacto-RGD identifies the level of integrin αvβ3 expression in man. *Clin Cancer Res.* 2006;12:3942–3949.
36. Beer AJ, Pelisek J, Heider P, et al. PET/CT imaging of integrin $\alpha_v\beta_3$ expression in human carotid atherosclerosis. *JACC Cardiovasc Imaging.* 2014;7:178–187.